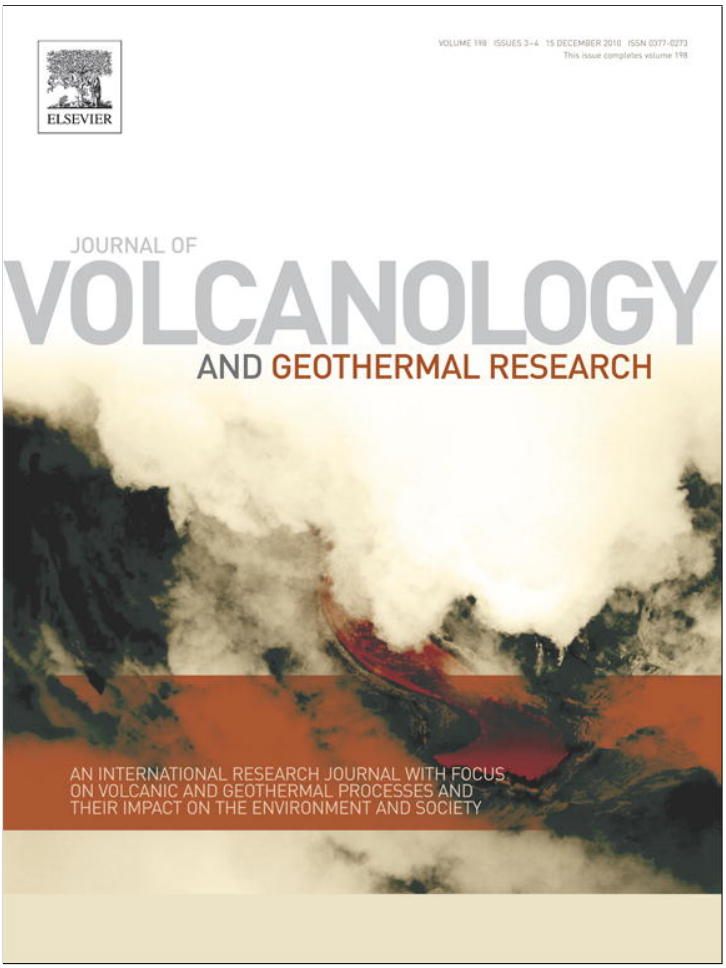

Journal of Volcanology and Geothermal Research 198 (2010) 288–296

Contents lists available at ScienceDirect

Journal of Volcanology and Geothermal Research

journal homepage: www.elsevier.com/locate/jvolgeores

Geochemical evidence for deep mantle melting and lithospheric delamination as the origin of the inland Damavand volcanic rocks of northern Iran

H. Mirnejad [a,*], J. Hassanzadeh [b], B.L. Cousens [c], B.E. Taylor [d]

[a] Department of Geology, Faculty of Science, University of Tehran, Tehran 14155-64155, Iran
[b] Division of Geological and Planetary Sciences, California Institute of Technology, Pasadena, CA 91125, USA
[c] Department of Earth Sciences, Carleton University, Ottawa, Ontario, K1S 5B6, Canada
[d] Geological Survey of Canada, 601 Booth Street, Ottawa, Ontario, K1A 0E8, Canada

ARTICLE INFO

Article history:
Received 16 February 2010
Accepted 9 September 2010
Available online 17 September 2010

Keywords:
Damavand
delamination
Neo-Tethys
partial melting
deep mantle

ABSTRACT

The intraplate Damavand volcanic field that overlies the Alborz Mountains in northern Iran is dominantly comprised of trachyandesite and alkali olivine basalt. Alkali olivine basalt is the most primitive rock type among Damavand lavas and exhibits a number of geochemical characteristics (e.g., high MgO, Ni and Cr abundances) that preclude substantial differentiation and crustal contamination. The lavas are light rare earth element enriched and have small negative Nb–Ta–Ti and positive Ba and Pb anomalies. The initial Nd and Sr isotope compositions of these lavas plot within the mantle array and cluster near bulk silicate Earth-values, while Pb isotope ratios are typical of modern upper crust. Oxygen isotope ratios range from +6.5 to +6.9‰. Although previous studies suggest that the mantle source of the Damavand volcanic rocks was metasomatized by the release of fluids during Tertiary subduction of Neo-Tethys oceanic crust under the Iranian Plate, the geochemistry of the alkali olivine basalts (e.g., BSE-like Sr and Nd isotopic compositions; the position of samples on Ti/V vs. Zr/Nb, Ce/Pb vs. Ce, and Th–Ta–Hf diagrams) is not reconcilable with derivation of the parental magma from such a mantle source. In addition, the Mid-Ocean Ridge Basalt (MORB) normalized trace element patterns of the Damavand alkaline olivine basalts most resemble those of Ocean Island Basalt (OIB) that implies the role of deep mantle source in their genesis. It seems that local upwelling of deep mantle materials underneath the Alborz Mountains resulted in the eruption of intraplate Damavand lavas. Compressional stress exerted on the Iranian plate following Neo-Thetys closure was the likely cause of sub-continental lithosphere delamination which led to such local mantle upwelling.

1. Introduction

Continental volcanic rocks can provide important information about paleo-geodynamic settings and the processes controlling the geochemical evolution of the sub-continental mantle. However, systematic studies of igneous rocks and the chemical composition of the mantle underlying the Iranian continental plate are few in number. The Damavand volcano, a Plio-Pleistocene volcanic center in north-central Iran, rises to an elevation of 5670 m and covers an area of approximately 800 km^2 (Fig. 1). The results of K/Ar, ^{40}Ar/^{39}Ar and (U–Th)/He dating methods suggest that Damavand volcanism has occurred frequently from the Late Pliocene to the Holocene (Davidson et al., 2004; Liotard et al., 2008).

The nature of the source region for Damavand magmatism is a matter of considerable controversy. Jung et al. (1976), Brousse and Moine-Vaziri (1982), and Aftabi and Atapour (2000), based on petrography and major element compositions, attributed Damavand volcanic activity to Cenozoic Neo-Tethys oceanic subduction under central Iran. Mehdizadeh et al. (2002) and Liotard et al. (2008) suggest that the source of the Damavand lavas is a metasomatized mantle, modified by subduction process. Davidson et al. (2004) consider that the initiation of Damavand intraplate volcanic activity was associated with local hotspot. However, the nature of mantle source enrichment as well as the mechanism of subduction beneath Damavand volcano has not yet been discussed. Our study presents major and trace element data and Sr, Nd, Pb and O isotope compositions for a number of volcanic rocks from Damavand, with the aim of addressing the nature of the mantle source and evaluating the role of convergent margin versus intraplate processes in their genesis.

2. Geology

The Alborz Mountain Range is a 600 km long and 100-km-wide east–west trending fold and thrust belt that stretches across northern Iran and south of the Caspian Sea (Fig. 1). The bedrock consists of a Paleozoic–Mesozoic passive-margin sedimentary sequence with few

* Corresponding author. Tel.: +98 21 6111 2959; fax: +98 21 6649 1623.
E-mail address: mirnejad@khayam.ut.ac.ir (H. Mirnejad).

0377-0273/$ – see front matter © 2010 Elsevier B.V. All rights reserved.
doi:10.1016/j.jvolgeores.2010.09.014

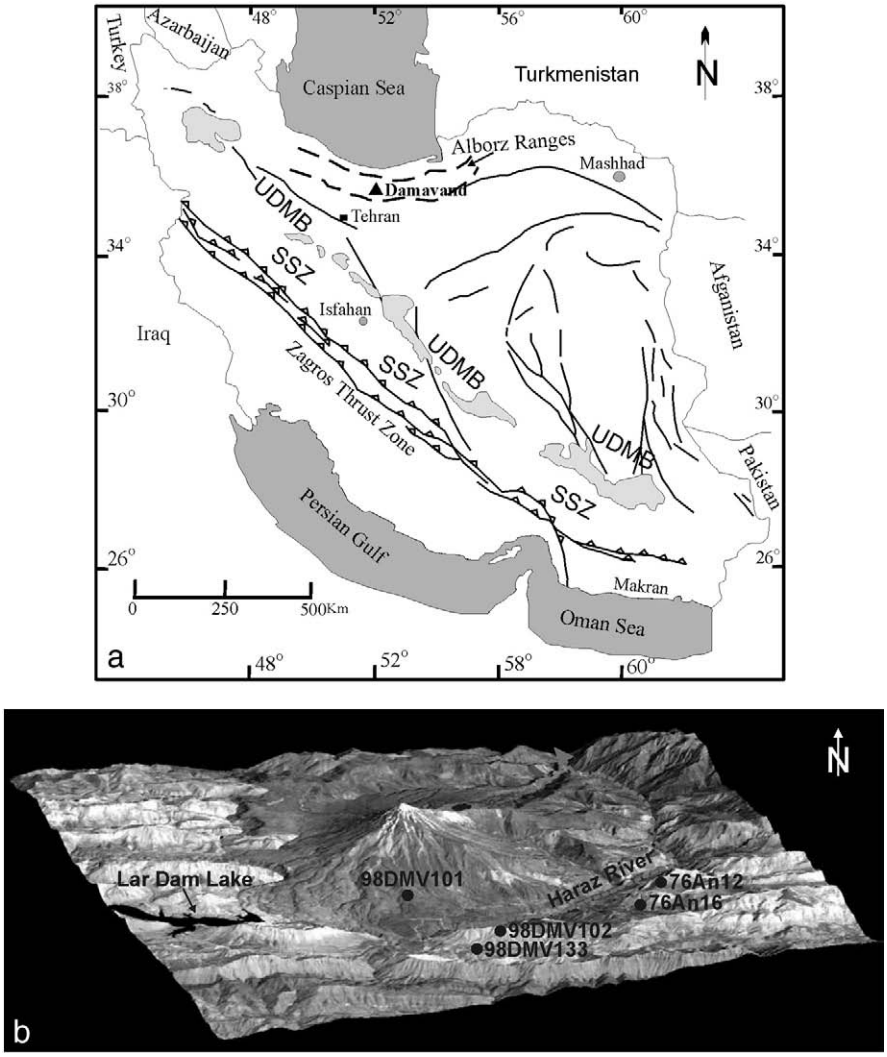

Fig. 1. (a) Map of Iran showing the position of the Damavand volcano, with respect to the Alborz Ranges, Urumieh–Dokhtar magmatic belt (UDMB), and Sanandaj–Sirjan zone (SSZ). (b) The position of collected samples on a satellite photo from Damavand.

volcanic rocks, overlain, in the south, by Tertiary volcanics and sediments. The Alborz is seismically active as it accommodates near 25% of the whole Arabian–Eurasian convergence in Iran (Vernant et al., 2004). Recent fault movements are mainly reverse with range-parallel sinistral component (Jackson et al., 2002) although sense of the strike-slip offsets was just the opposite before ca. 5 ± 2 Ma (Axen et al., 2001).

According to Sengör et al. (1993) and Zanchi et al. (2006), the Alborz range results from different tectonic events, which occurred during two major orogenic cycles: (1) the Late Triassic (Cimmerian) demise of the Paleotethys and collision of the Iranian block with Eurasia; and (2) the post-Neo-Tethys, intraplate deformation related to the convergence of the Arabian and the Eurasian plates. The final closure of Neo-Tethys and suturing of the Afro-Arabian and Iranian plates are recorded in the Zagros orogenic belt, part of the Alpine–Himalayan orogenic belt that extends from Europe, through Iran, to western Pakistan. From SW to NE four main structural units comprise the Zagros orogenic belt: Zagros folded belt, Crush zone (High Zagros), the Sanandaj–Sirjan zone (SSZ), and the Urumieh–Dokhtar magmatic belt (UDMB) (Stöcklin, 1968; Braud and Ricou, 1971; Berberian and King, 1981; Bina et al., 1986; Alavi, 1994; Agard et al., 2005).

Damavand volcano, located in the central part of Alborz Mountains, is a large composite cone that consists of mainly trachyandesite lava flows, and subordinate pyroclastic materials (Davidson et al., 2004). The immediate basement to Damavand volcano in the Alborz Mountains is a folded and thrust-faulted passive-margin sedimentary sequence of carbonate, siliciclastic, and volcanic rocks. Young normal faulting attributed to transtension has been documented in central Alborz (Ritz et al., 2006) and around the Damavand (Hassanzadeh et al., 2006; Omidian, 2007).

3. Analytical techniques

Fresh samples of alkali olivine basalt (98DMV-101, -102, -133; Table 1), and trachyandesite (76An-2, -3) were collected from the peripheral Damavand cinder cone and the south east side of Haraz River, respectively (Fig. 1). Whole-rock major and trace element compositions were determined using inductively plasma optical emission spectrometry (ICP-OES) and inductively plasma mass spectrometry (ICP-MS) at Geosciences laboratories, Sudbury, Ontario. All samples for ICP analysis were dissolved using an alkali fusion ($LiBO_2/LiB_4O_7$) method. Reproducibility, based on repeat analyses, for the major elements is ±1.0% of the quoted values, while most trace elements have an uncertainty of ±5.0% for the concentrations >100 ppm, and ±10% for those with concentrations <100 ppm.

Radiogenic isotopic analyses were performed on whole-rock powders, digested in closed Savillex beakers using ultrapure HF and HNO_3 in a proportion of 2:5, and heated for 48 h to ensure complete

Table 1
Chemical composition of samples from Damavand volcanic field.

Sample #	98DMV101	98DMV102	98DMV133	76-An-12	76-An-16
SiO_2 wt.%	45.61	47.57	46.98	62.60	60.63
TiO_2	2.05	1.74	1.87	0.90	1.07
Al_2O_3	12.85	13.96	13.79	15.56	15.90
MgO	8.47	8.22	8.46	2.15	2.76
CaO	9.49	8.09	8.28	3.55	4.36
MnO	0.12	0.12	0.12	0.05	0.07
FeO	6.29	6.09	6.11	1.63	2.79
Fe_2O_3	3.00	2.90	2.91	1.21	2.07
Na_2O	5.06	3.70	4.01	4.56	4.78
K_2O	1.91	2.84	3.67	4.61	4.36
P_2O_5	1.57	1.19	1.45	0.53	0.62
LOI	2.30	2.20	0.10	2.46	0.52
SUM	96.74	96.60	97.94	98.20	98.53
V ppm	139	140	142	121	9
Cr	281	254	290	58	88
Ni	229	205	227	106	99
Rb	42	47	62	60	55
Sr	2209	1860	2156	1914	1933
Y	17	17	17	12	13
Zr	334	305	372	352	320
Nb	77	53	61	57	54
Cs	2.36	1.42	1.41	0.75	0.66
Ba	2368	1466	1941	1269	1282
La	123	102	114	87	102
Ce	205	201	243	195	181
Pr	>25	22.88	>25	22.46	22.59
Nd	94	74	97	71	79
Sm	13.17	11.59	14.51	10.33	11.64
Eu	4.07	3.36	4.39	3.01	3.03
Gd	8.51	8.48	10.06	7.39	7.92
Tb	1.07	1.02	1.22	0.89	0.92
Dy	4.75	4.72	5.34	4.05	4.02
Ho	0.86	0.86	0.92	0.69	0.72
Er	2.17	2.19	2.21	1.73	1.82
Tm	0.32	0.29	0.30	0.25	0.24
Yb	1.82	1.68	1.72	1.53	1.48
Lu	0.29	0.26	0.28	0.20	0.22
Hf	7.70	6.80	8.10	7.60	7.30
Ta	4.35	2.95	3.30	2.84	2.74
Pb	15.80	12.60	13.90	13.80	12.90
Th	8.56	9.92	9.93	10.58	9.81
U	2.35	2.60	2.84	2.67	2.21
$\delta^{18}O$	6.80	6.47	6.52	6.86	6.63
$^{87}Sr/^{86}Sr$	0.70431	0.70447	0.70446	0.70500	0.70500
$^{143}Nd/^{144}Nd$	0.51266	0.51268	0.51265	0.51260	0.51262
$^{206}Pb/^{204}Pb$	18.733	18.672	18.744	18.804	18.796
$^{207}Pb/^{204}Pb$	15.620	15.599	15.624	15.644	15.651
$^{208}Pb/^{204}Pb$	38.873	38.758	38.839	38.956	38.959

98DMV101, 98DMV102, 98DMV133: alkali olivine basalt; 76-An-2, 76-An-16: trachyandesite.

digestion. The elements Rb, Sr, REE and Pb were separated using ion-exchange chromatography (see Cousens, 1996; Cousens et al., 2003). The average values of total procedural blanks obtained during the time that this work was done are as follow: Rb 0.5 ng, Sr 1.5 ng, Sm 0.04 ng, Nd 0.26 ng and Pb 1 ng. Strontium, Nd, and Pb isotope ratios were measured on a Finnigan-MAT 261 mass spectrometer at Carleton University, operated in the static mode. On the basis of numerous runs collected during the course of this work, average values (and respected 2σ uncertainties) for the isotopic ratios of the following standards were: NBS-987 $^{87}Sr/^{86}Sr = 0.710251 \pm 0.000020$, La Jolla $^{143}Nd/^{144}Nd = 0.511870 \pm 0.000020$, NBS 981 $^{206}Pb/^{204}Pb = 16.890 \pm 0.010$, $^{207}Pb/^{204}Pb = 15.429 \pm 0.013$, and $^{208}Pb/^{204}Pb = 36.498 \pm 0.042$. Measured Sr and Nd isotope ratios for unspiked samples were corrected for fractionation using $^{88}Sr/^{86}Sr = 8.3752$ and $^{146}Nd/^{144}Nd = 0.7219$. An average correction for fractionation of $0.12 \pm 0.01\%$ per mass unit was applied to all measured Pb isotope ratios on the basis of results for NBS 981. For some samples, Sm, Nd, Rb, and Sr abundances were measured by isotope dilution with uncertainties of <0.5%.

For O isotope analysis, approximately 7 mg of whole-rock powders was oven-dried for 24 h. Samples were then transferred to Ni bombs and fluorinated with BrF_5 (e.g., Taylor, 2004). The Ni bombs were heated to 600 °C for 12 h. The extracted O_2 was converted to CO_2 and then measured on a Finnigan-MAT 252 multi-collector mass spectrometer at the Geological Survey of Canada, Ottawa. The $\delta^{18}O$ values are reported relative to V-SMOW with a reproducibility of $2\sigma \pm 0.2‰$, based on multiple runs of NCSU-Qtz, an in-house standard quartz.

4. Petrography and geochemistry

The petrography of the volcanic rocks along with the geology and physical volcanology of the Damavand volcanic center has been previously described by Pandamouz (1998), Ashrafi (2003), Davidson et al. (2004) and Liotard et al. (2008). Only a brief description of the samples studied is given here. The alkali basalts are vesicular and have porphyritic textures, with microphenocrysts of olivine (15%), and clinopyroxene (10%) and laths of plagioclase set in a matrix of olivine, clinopyroxene, plagioclase and opaque minerals. Olivine crystals are euhedral to subhedral and unzoned. The trachyandesites have microphenocrysts of apatite (1%), biotite (5%) and plagioclase (up to 50%) residing in a matrix of clinopyroxene, plagioclase, and opaque minerals. Plagioclase shows concentric and complex zonation, and some grains have undergone sericitic alteration. It should be noted that some authors classified the volcanic rocks from Damavand as absarokite and banakite (Brousse and Moine-Vaziri, 1982; Liotard et al., 2008), but for simplicity and for the purpose of this paper, we classify these rocks as alkali olivine basalt and trachyandesite, respectively (cf. Pandamouz, 1998; Ashrafi, 2003; Davidson et al., 2004).

The results of the geochemical analyses of the Damavand volcanic rocks are presented in Table 1. Major element totals are low for the alkali olivine basalts. Plots of MgO (wt.%) vs. other major element oxides (Fig. 2) reveal a negative correlation of MgO with SiO_2, but broadly positive correlations between MgO and CaO, and TiO_2. The alkali olivine basalts have lower $Na_2O + K_2O$ contents relative to trachyandesites (Fig. 1).

The chondrite-normalized (McDonough and Sun, 1995) rare earth element (REE) patterns of Damavand lavas show enrichment in light REE (LREE) relative to heavy REE (HREE) (Fig. 3). Alkali olivine basalts and trachyandesites have, respectively, the highest and lowest REE concentrations. The REE patterns flatten through the middle to heavy REE. In a MORB-normalized (Weaver, 1991) trace element plot (Fig. 4), all samples display enrichments in large ion lithophile elements (LILE), LREE and Pb, and depletions in Nb, Ta and Ti. The trachyandesites have lower LILE and high field strength elements (HFSE) than the alkali basalts, but are more enriched in U and Th. The position of the alkali olivine basalts, the most primitive rocks from Damavand on plots of Ti/V vs. Zr/Nb, Ti/Y vs. Nb/Y and Ce/Pb vs. Ce binary as well as Th–Ta–Hf ternary diagrams is shown in Fig. 5.

In a Nd–Sr isotope plot diagram (Fig. 6), alkali olivine basalts plot close to Bulk Silicate Earth (BSE) whereas trachyandesites have higher $^{87}Sr/^{86}Sr$ ratios and lower $^{143}Nd/^{144}Nd$ ratios and plot within the more enriched parts of the diagram. The range of variations in Pb isotope ratios is small for the analyzed samples, yet the trachyandesites have slightly higher Pb isotope ratios than the alkali olivine basalts. Note that they all plot above the Northern Hemisphere Reference Line (NHRL), and very close to the geochron and the Stacey–Kramer's (Stacey and Kramer, 1975) crustal Pb isotope evolution curve (Fig. 7). Whole-rock oxygen isotope compositions for alkali olivine basalts ($\delta^{18}O = +6.5$ to $+6.8‰$) are similar to those of the more evolved trachyandesites ($\delta^{18}O = +6.6$ to $+6.9‰$). Oxygen isotope ratios are all just above the range for the upper mantle (Mattey et al., 1994) but do not show correlations with any particular major and trace elements, nor with other isotopes.

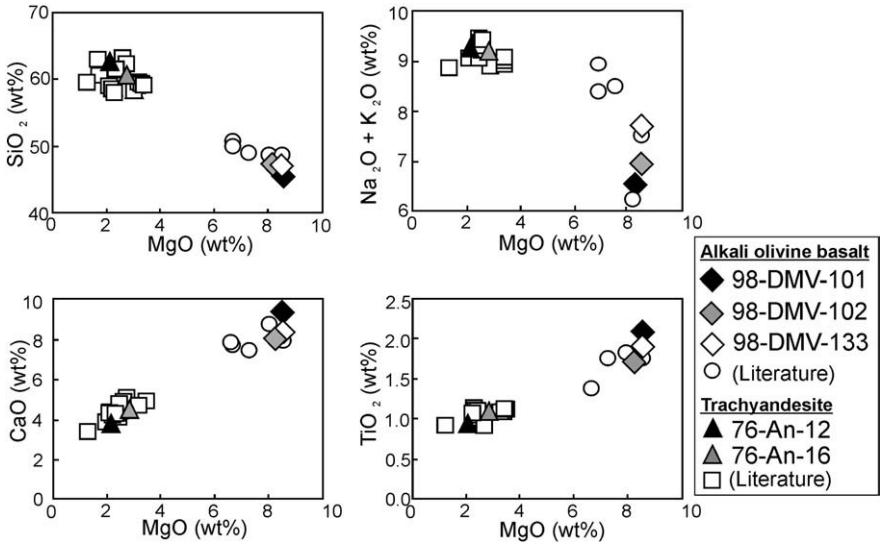

Fig. 2. Whole-rock major element plots of volcanic rocks from Damavand. Open circles and rectangles represent literature data reported by Mehdizadeh et al. (2002), Davidson et al. (2004), and Liotard et al. (2008). Correlations between the major element contents are consistent with a genetic relationship between samples.

5. Discussion and conclusions

5.1. The primary nature of Damavand lavas

Alkali olivine basalts from Damavand have characteristically low SiO_2 contents (ca. 47 wt.%) and elevated MgO (ca. 8 wt.%), Ni (182–229 ppm) and Cr (259–345 ppm) abundances (Table 1) that indicate they are the most primitive among the Damavand lavas and thus have been possibly derived by partial melting of ultramafic sources. It is conceivable that enrichment of incompatible trace elements such as Ba, Rb, La and Ce in alkali olivine basalts (Fig. 4) resulted from contamination of magmas with crustal materials. However, alkali olivine basalts have higher LILE and LREE abundances than average Upper Continental Crust (Fig. 4) and therefore crustal contamination is not likely to have a discernable impact on the chemical composition of magma. Also, the Sr and Nd isotope ratios of Damavand alkali olivine basalts plot in the mantle array, furthest from the likely isotopic compositions of older Iranian continental crust (Fig. 6). Although the Pb isotope ratios and the slightly elevated $\delta^{18}O$ values of alkali olivine basalts may argue that these lavas include small proportion of an evolved component, the high MgO, Ni and Cr contents do not support extensive crustal contamination during magma ascent. Thus the geochemical signatures of the Damavand alkali olivine basalts can be used to constrain the nature of their mantle source.

Trachyandesites are the most evolved rock types in Damavand, and the positions of their plotted compositions on various geochemical diagrams (Figs. 2–4) suggest that they are somehow related to the more mafic alkali olivine basalts. Mass balance calculations by Liotard et al. (2008) show that trachyandesites can be derived from the alkali olivine basalt following ~70% crystal fractionation of cumulate minerals including olivine, clinopyroxene, plagioclase, biotite, Ti-magnetite and apatite. Trachyandesites, in addition to having higher SiO_2, lower MgO and higher LILE contents compared to those of the alkali olivine basalts, have higher Sr and lower Nd isotope ratios that clearly indicate crustal assimilation accompanied by the fractional crystallization (AFC; DePaolo, 1981) has played an important role in modifying the chemical composition of the former lava in Damavand. Liotard et al. (2008) have demonstrated that 6–7% contamination of alkali olivine basalts with upper crust granitoids can lead to the generation of a magma having Sr, Nd and Pb isotopic compositions similar to those of the Damavand trachyandesite. However, the amount of crystal fractionation as well as crustal assimilation of alkali olivine basalt to create trachyandesite should be treated with caution because 70% fractionation of an assemblage, including plagioclase, as well as 6–7% assimilation of a granitoid is expected to impact the trace element patters of trachyandesite, increase the $\delta^{18}O$ values substantially, and create significant Eu anomaly.

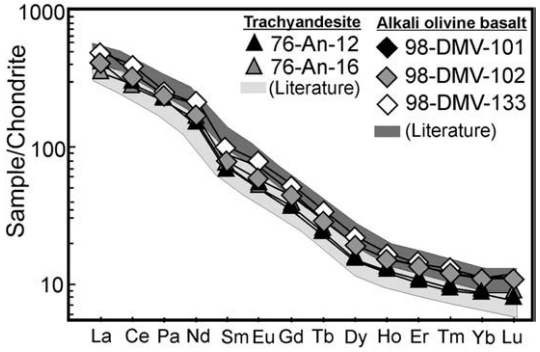

Fig. 3. Chondrite-normalized (see McDonough and Sun, 1995) REE patterns of the Damavand volcanic rocks. The alkali olivine basalts contain the highest concentrations of REE. The light and dark gray areas cover the data reported by Mehdizadeh et al. (2002) and Liotard et al. (2008).

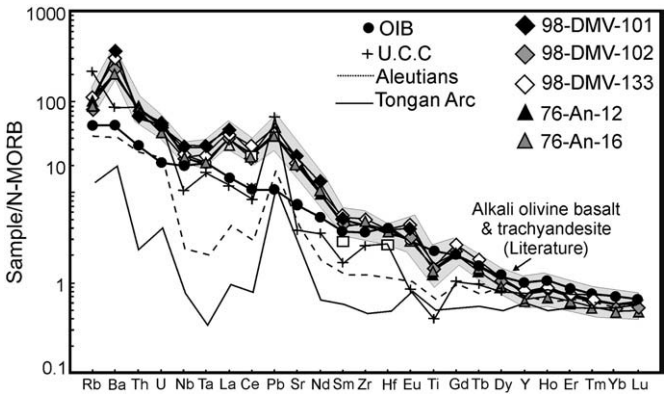

Fig. 4. N-MORB-normalized (see Weaver, 1991) trace element patterns for the Damavand volcanic rocks. OIB = Ocean Island Basalts, U.C.C = Upper Continental Crust. Trace element pattern of volcanic rocks from Aeolian arc and Sunda arc is presented for comparison. The light gray area shows trace element data reported by Mehdizadeh et al. (2002) and Liotard et al. (2008).

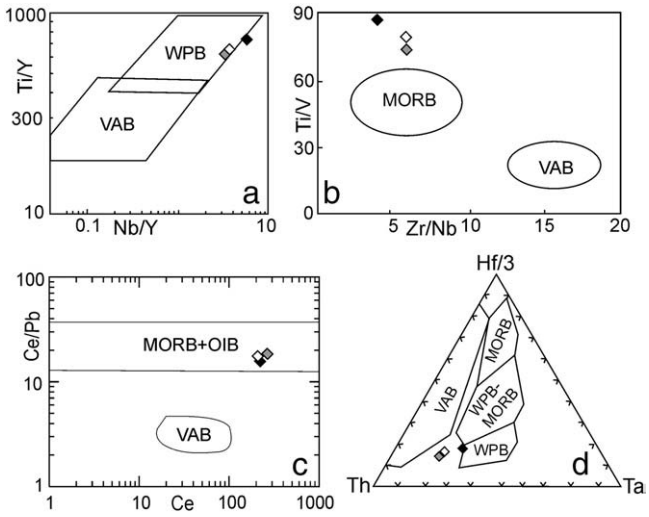

Fig. 5. (a) Ti/Y vs. Nb/Y (see Pearce, 1982), (b) Ti/V vs. Zr/Nb (see Verdel, 2009), (c) Ce/Pb vs. Pb (see Pearce, 1982), and (d) Th–Hf–Ta (see Wood, 1980) discrimination diagram for Damavand alkali olivine basalts. VAB = Volcanic Arc Basalts, MORB = Mid-Ocean Ridge Basalts, WPB = Within Plate Basalts. Symbols as in Fig. 3. Alkali olivine basalts are the only unfractionated lavas in Damavand that originated from a primary magma, and are therefore the most suitable samples for tectonic discrimination diagrams.

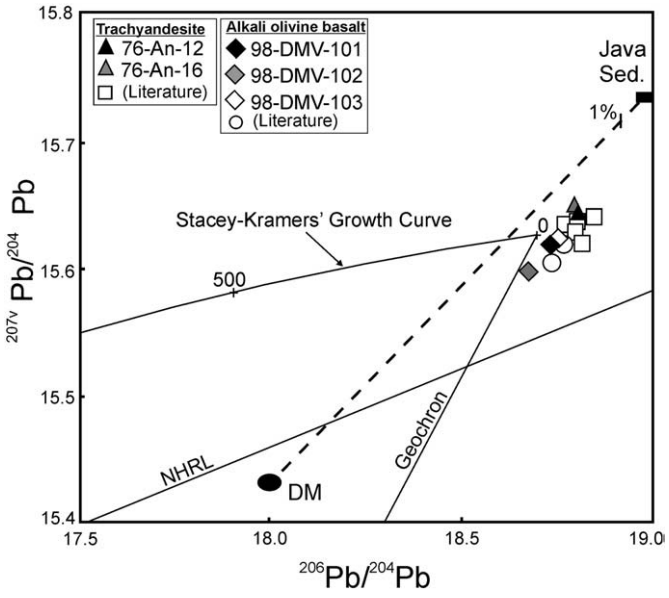

Fig. 7. $^{207}Pb/^{204}Pb$ versus $^{206}Pb/^{204}Pb$ diagram showing Pb isotope ratios for the Damavand volcanic rocks. The data plot very near the geochron and the Stacey–Kramer's (Stacey and Kramer, 1975) model curve for average crustal Pb isotope evolution and above the Northern Hemisphere Reference Line (NHRL). Trachyandesites have higher Pb isotope ratios relative to the alkali olivine basalts. Numbers on the growth line indicate the date in Ma. Addition of a small amount (1%) of pelagic sediments to a depleted mantle source can significantly increase the Pb isotope ratios. Open circles and rectangles represent data reported by Liotard et al., 2008.

5.2. Neo-Tethys oceanic crust subduction underneath Damavand volcanic field

The geochemical characteristics of the Damavand alkali olivine basalts led Mehdizadeh et al. (2002) and Liotard et al. (2008) to suggest that an enrichment event must have modified the mantle source prior to the initiation of partial melting. Metasomatic agents affecting the mantle sources may have included either volatile-rich partial melts or H_2O–CO_2 fluids that originated from the dehydration or partial melting of subducted slabs (Menzies and Hawkesworth, 1987; Hawkesworth et al., 1990) or from plume heads (McKenzie, 1989; Tainton and McKenzie, 1994). A number of geochemical peculiarities of Damavand lavas such as Nb, Ta, and Ti depletions,

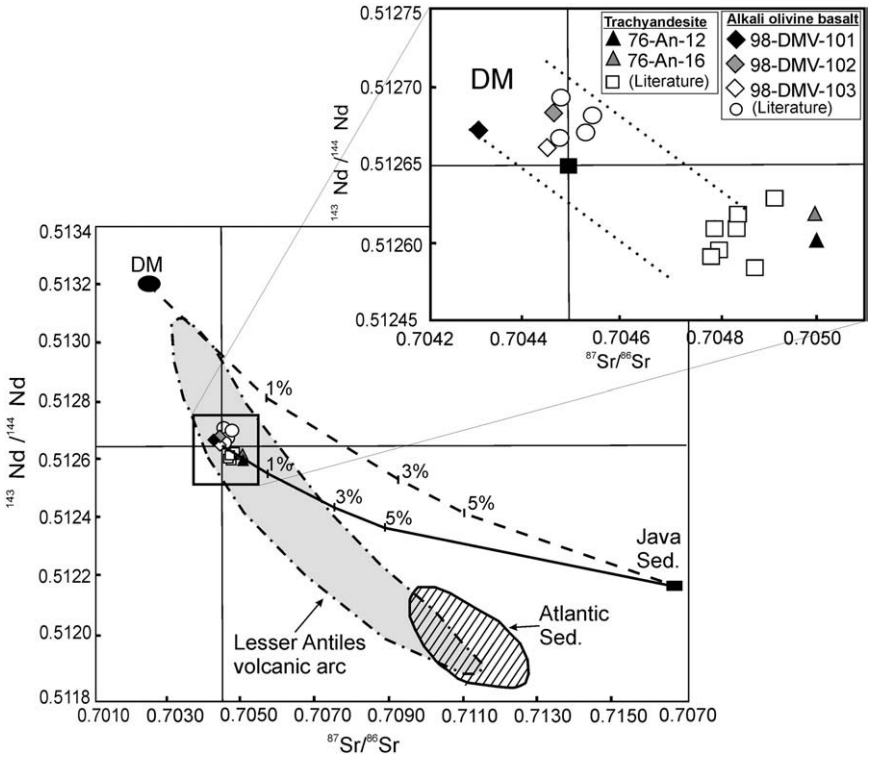

Fig. 6. $^{143}Nd/^{144}Nd$ and $^{87}Sr/^{86}Sr$ isotope variation diagram for Damavand volcanic rocks. Numbers on the lines specify the percentage of pelagic sediment (see Plank and Langmuir, 1998) which was added to either a depleted (see Rehkamper and Hofmann, 1997) or pristine mantle source. Inset shows in details the Nd and Sr isotopic compositions of Damavand lavas. The data from the alkali olivine basalts plot within the mantle array (dotted lines) and close to the field of BSE (Bulk Silicate Earth) mantle component (filled square). Open circles and rectangles represent data reported by Liotard et al., 2008. DM = Depleted mantle. Data for Lesser Antilles volcanic rocks and Atlantic sediments after Wilson (2001).

LILE enrichment, positive Ba and Pb anomaly as well as their similarity to the shoshonitic series lavas were regarded as a ubiquitous subduction zone signature by Mehdizadeh et al. (2002) and Liotard et al. (2008). These authors also indicated that the enrichment event was related to subduction of either the ocean-like Caspian crust to the southwest or the Paleo-Tethyan subduction, induced by the Zagros formation, to the northeast. Recently published studies suggest, on the contrary, that the northwest extrusion of the South Caspian region was accommodated by subduction beneath the north Caspian region to the north (Axen et al., 2001; Allen et al., 2002; Allen et al., 2003; Ritz et al., 2006; Hollinsworth et al., 2008). In addition, a number of studies on the geodynamic of the Paleo-Tethys demonstrate that Paleo-Tethys oceanic crust subducted northward from Late Devonian to Late Triassic time underneath the Turan Plate. Rather than involving Paleo-Tethys, Jung et al. (1976), Brousse and Moine-Vaziri (1982), and Aftabi and Atapour (2000) have attributed the Damavand volcanic activity to Cenozoic Neo-Tethys oceanic subduction under Central Iran, and argue that the increasing K_2O content of volcanic rocks from the UDMB to Damavand volcano may reflect the depth to a Benioff zone, increasing northward in a manner analogous to the "K–h" relationship of Dickinson and Hatherton (1967).

One of the most important parameters that determine the chemical composition of the arc magma source is the composition and quantity of the components involved (the mantle wedge, fluids from the hydrated oceanic crust, and subducted sediments). In the case of the Damavand volcanic field, the dominant mantle end-member prior to metasomatism could have been either a depleted or primitive mantle source. Contributions of subducted sediments to such a mantle wedge have been revealed by many geochemical studies of volcanic rocks from arc settings (e.g., Gill and Williams, 1992). Plank and Langmuir (1998) have compiled trace element and/or isotope data from a variety of subducting sediments including those of Makran and Java. Close examination of such data shows that oceanic sediments from Makran and Java are very similar in terms of trace element abundances. Fig. 8 illustrates incompatible trace element patterns generated by mixing between subducted sediments and a presumed depleted mantle source. The chemical compositions of mixing components are given in Table 2. Our modeling demonstrates that various amounts of pelagic sediments added to a depleted mantle fail to create trace element patterns similar to those of the Damavand alkali olivine basalt (Fig. 8). More importantly, addition of such amount of pelagic sediments changes the Sr, Nd and Pb isotopic ratios of a depleted mantle source to levels significantly different from those of the Damavand alkali olivine basalt (Figs. 6 and 7). Trace element modeling by Liotard et al. (2008) suggests that the source of

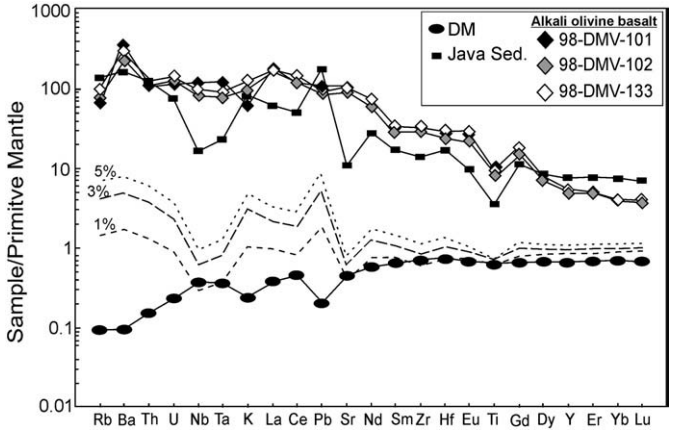

Fig. 8. Primitive mantle-normalized (see McDonough and Sun, 1995) diagram showing the compositions of a depleted mantle source component (see Workman and Hart, 2005) contaminated with 1%, 3% and 5% of subducted Java pelagic sediment (see Plank and Langmuir, 1998).

Table 2
Average chemical composition of depleted mantle source (Rehkamper and Hofmann, 1997; Workman and Hart, 2005) and Java pelagic sediments (Plank and Langmuir, 1998), used for mixing callucation.

	Java sed.	DM
TiO_2	0.71	0.12
K_2O	2.50	0.00
Rb	0.05	82.10
Sr	6.09	218.00
Y	3.33	32.60
Zr	5.08	145.00
Nb	0.09	10.92
Ba	0.56	1068.00
La	0.25	39.08
Ce	0.55	86.08
Nd	0.58	33.95
Sm	0.24	7.06
Eu	0.10	1.43
Tb	0.36	6.23
Dy	0.51	5.66
Er	0.35	3.35
Yb	0.37	3.24
Lu	0.06	0.48
Hf	0.16	4.73
Ta	0.01	0.85
Pb	0.01	25.50
Th	0.01	9.78
U	0.00	1.47
$^{87}Sr/^{86}Sr$	0.70	0.72
$^{143}Nd/^{144}Nd$	0.51	0.51
$^{206}Pb/^{204}Pb$	18.00	18.99
$^{207}Pb/^{204}Pb$	15.43	15.74

Damavand alkali olivine basalts (their absarokites) was likely a metasomatized lherzolite. However, our mixing calculations also show that the Sr and Nd isotope ratios of a primitive lherzolite mantle source contaminated by small amounts of subducted pelagic sediments (<0.5%) are substantially higher than those of young Damavand basalts (Fig. 6). On Nd vs. Sr isotope diagram, these basalts do not show a mixing trend between depleted mantle components and subducted sediments, as exhibited by the volcanic rocks from the Lesser Antilles (Fig. 6). It should also be mentioned that some authors (e.g., Davidson, 1996) who would argue that the extreme compositions from the Lesser Antilles are crustal contamination. Additionally, the limited ranges of $\delta^{18}O$ (i.e., +6.5 to +6.8‰) in alkali olivine basalts argue against contributions from subducted materials in the mantle source of Damavand volcanic rocks. Pineau et al. (1999) have shown that higher scatter $\delta^{18}O$ range from 5.3 to 8.5‰ in lavas from Kamtchatka Peninsula, far-east Russia, is inherited from mixtures of normal mantle magmas with a slab-derived, water-rich fluid/magma. A quantitative modeling by Eiler et al. (2000) and Eiler (2001) also demonstrated that addition of ^{18}O-enriched slab-derived fluids or melts to an upper mantle with $\delta^{18}O = 5.5‰$ can create lavas highly scattered in $\delta^{18}O$. The calculations by these authors, furthermore, predicted a strongly hyperbolic covariation of $\delta^{18}O$ values and $^{87}Sr/^{86}Sr$ ratios. Close examination of isotopic data (Table 1), reveals that such isotopic correlations cannot be found among alkali olivine basalts from Damavand. Although depletions in Nb, Ta, Zr and Ti are normally considered as geochemical evidence for subduction-related magmatism, because the metasomatic agents that originate from within the subducted oceanic crust are deficient in these elements (Proteau et al., 2001), these are also characteristics of the continental crust. Moreover, the trace element patterns and the degree of LILE enrichment of alkali olivine basalts in Damavand are different from typical arc magmas, including Aleutians and Tongan Arc (Fig. 4). The depletions in Nb, Ta, Zr and Ti in the Damavand volcanic rocks could well result from either the retention of Ti-bearing phases in the mantle source or the slight reaction of the magma with the crustal materials, both unrelated to subduction activity. On plots of Ti/V vs. Zr/Nb, Ti/Y vs. Nb/Y and Ce/Pb vs. Ce binary as well as Th–Ta–Hf

ternary tectonic discriminant diagrams, which are only valid for the primitive rocks, the alkali olivine basalts from Damavand plot well away from arc settings (Fig. 5). Also, these lavas not only do not plot on orogenic field but also are restricted to the anorogenic domain on Th/Yb vs. Ta/Yb and Th*1000/Zr vs. Nb*1000/Zr tectonic discriminant diagrams (not shown). Along with the afore-mentioned geochemical considerations, the distance of the Damavand volcanic rocks from the Zagros Trench (ca. 400 km) and its age relation (1.8 Ma–7 ka) to the Neo-Tethys closure (20 Ma) are problematic when trying to relate the Damavand magmatism to Neo-Tethys subduction.

Although the distance of the Damavand volcanic rocks from the Zagros Trench can be resolved by the low angle subduction of oceanic crust, as has been invoked to explain inland volcanism in western North America (Feeley, 2003; Murphy et al., 2003) and Andean margins (Gutscher et al., 2000), recent studies on magmatism in SSZ and UDMB reveal that subduction of the Neo-Thetys slab occurred much earlier than the time of Damavand volcanism (Agard et al., 2005; Shafiei et al., 2009; Verdel, 2009). Igneous rocks from SSZ and UDMB formed during two distinct episodes: Jurassic–Cretaceous and Tertiary, respectively (Beberian and Beberian, 1981; Agard et al., 2005; Ahmadi-Khaladj et al., 2007), suggesting that the axis of magmatism shifted 300 km to the northeast from its initial position within the SSZ at the end of Mesozoic. Because geochemical data of Mesozoic and Tertiary igneous rocks from the SSZ and UDMB are very similar and no continuous suture zone exist between these two, Omrani et al. (2008) and Verdel (2009) concluded that magmatism shifted from the SSZ to the UDMB in late Cretaceous as the result of the flat-slab subduction of the Neo-Thetys. The slab then broke off and subducted with a steep slope into the mantle underlying UDMB. Such subduction resulted in the Eocene to Late Miocene arc magmatism in the UDMB (Omrani, 2008). Keskin (2003) have also suggested similar model of Neo-Tethys slab steepening and break-off beneath Anatolia Plateau for magma generation in eastern Turkey. Agard et al. (2005) and Omrani et al. (2008) stress that any Plio-Quaternary magmatic activity to the north of the central UDMB is unrelated to subduction activity, because the last pieces of the Neo-Tethys oceanic slab sank into the mantle underlying the central parts of the UDMB (Omrani et al., 2009). The presence of linear and narrow arc magmatism along the strike in UDMB, which reflects a slab break-off and deep subduction in the late Miocene, is inconsistent with the subduction of the Neo-Tethys under the Damavand in Quaternary. It is thus inevitable to look for other processes and activities rather than subduction and convergent margin for the genesis of the Damavand volcanic rocks.

5.3. Deep mantle melting and lithospheric delamination

Another mechanism to consider for inland magmatism is deep mantle melting and the delamination of sub-continental lithosphere, in response to the crustal shortening (e.g., Davies and Blanckenburg, 1995). Deep mantle melting as a source of alkaline igneous rocks has been proposed by a number of authors. For example, phase equilibria studies on lamproites from the Gaussberg lamproites in the East Antarctic shield (Murphy et al., 2002) point to partial melting of mantle materials in the transition zone or lower mantle. Elkins-Tanton and Grove (2003) also performed phase equilibrium experiments on high K olivine luecitite from central Sierra Nevada and suggested that the magma was derived from a hydrous source at depths of greater than 100 km within the mantle. It is further suggested by Elkins-Tanton and Grove (2003) that lithospheric delamination some time before the Pliocene led the source material to rise into the lithospheric dome and melted adiabatically to produce the high-potassium magmas. Geophysical (Wernicke et al., 1996; Boyd et al., 2004; Zandt et al., 2004), geological and petrological (Ducea and Saleeby, 1998; Manley et al., 2000; Ducea, 2001; Lee et al., 2001) evidence also link the Pliocene potassic volcanism in the southern and central Sierra Nevada to the lithospheric mantle delamination (van Kooten, 1980; Dodge et al., 1986; Feldstein and Lange, 1999; Farmer et al., 2002). Kay and Kay (1993) used criteria such as onset of mafic volcanism and a regional change in the stress system, to postulate a Pliocene episode of lithospheric delamination in the southern Puna. Gao et al. (2002) also suggest that wholesale replacement of lithospheric mantle (± lower crust) beneath the North China craton may require large-scale continental collision.

The Iranian part of the Alpine–Himalayan active tectonic belt is currently deforming at a high rate. Agard et al. (2005) reported a minimum estimate of the post-Miocene collisional shortening rate to be 5–9.3 mm/year. In the Alborz Mountains, a total shortening of 30 km at the longitude of Tehran since the early Pliocene (Allen et al., 2003) is attributed to the northward shortening between the central Iranian block and the Eurasian plate (Vernant et al., 2004). Nazari (2006) also estimated the total amount of shortening at about 38% for the Alborz, mainly occurred after Eocene. Such compressional stresses induced on the Iranian plate led to major earthquake activity (Motazedian, 2006) as well as periodic lithospheric delaminations (Agard et al., 2005; Omrani et al., 2008). In a more local scale like in Damavand, transtensional systems have developed along releasing fault bends and step-overs (Ritz et al., 2006; Hassanzadeh et al., 2006; Omidian, 2007).

Geophysical studies have revealed that a mantle lithosphere is almost completely absent beneath the Alborz Mountains (e.g., Sodoudi et al., 2009). Bouguer anomaly modeling estimated crustal thickness of 35–40 km under the central Alborz and stimulated the idea of root deficiency (Dehghani and Makris, 1984). A relatively thicker crust (45–46 km) was shown for the same region based on surface wave analysis of a few events (Asudeh, 1982) and receiver function analysis of teleseismic data (Doloei and Roberts, 2003). A more recent study by Sodoudi et al. (2009), based on receiver functions, indicates a crustal thickness of ~51–54 km beneath the range. Rajaee et al. (2010) reported an even thicker crust (55–58 km) indicating a moderate crustal root but still inadequate to compensate the existing elevation. The relatively thin crust for a 100 km wide, 3–5 km high mountain range has also been interpreted to be indicating lack of compensation by a lithospheric root (Guest et al., 2007). Inadequate crustal root and the relatively thin lithosphere beneath the Alborz may imply that asthenospheric mantle is supporting the high elevation (Sodoudi et al., 2009). Absence of a crustal root in the Alborz may be due to lower crustal flow and sub-continental delamination as speculated by Allen et al. (2003).The Damavand volcanic rocks could not have originated from a depleted upper mantle because the asthenosphere is depleted in incompatible trace elements and has dramatically different Sr, Nd, Pb and O isotope compositions. Therefore, partial melting of such an upper mantle source cannot produce a melt similar in chemical composition to that of the alkali olivine basalt from Damavand. Davidson et al. (2004) suggest that the geochemical constraints of Damavand volcanic rocks are in line with a local hotspot/plume origin, associated with lithospheric delamination. The Sr and Nd isotope data from the Damavand volcanic rocks plot within the field of mantle array which represents OIB (Fig. 6) and the trace elements patterns of Damavand alkali olivine basalts are also more similar to those of OIB (Fig. 4). The position of the studied samples around the Pb isotope crustal evolution curve (Fig. 7) which indicates a crustal source for Pb, along with the LILE-Pb enrichment and Nb–Ta depletions, however, can be explained by slight upper crustal contamination accompanied by small degrees partial melting of an OIB-like mantle source. Reagan and Gill (1989) have shown that incompatible trace element enrichment in magma can be inherited from small-degree partial melting of an OIB-like mantle source. Furthermore, numerical modeling by McKenzie (1989) and Tainton and McKenzie (1994) demonstrated that melts emanating from mantle upwelling can be enriched in volatiles and incompatible elements. It thus seems likely that partial melting of an OIB-like mantle source generated magma

with trace element contents similar to those of Damavand basalts. In this case, transtension probably provided conduits for mantle-derived magmas to ascend to the surface (Hassanzadeh et al., 2006; Omidian, 2007).

Since crustal thickening and shortening in response to the compression from the Afro-Arabian plate is an ongoing process, it is speculated that more examples of mantle delamination and within-plate magmatism could be found in parts of Iran located to the north of the Zagros suture zone, and beneath the Alborz Mountains.

Acknowledgments

We would like to thank the editor, Dr. M. J. Rutherford and anonymous reviewers for thorough reviews and comments. J. Davidson and J. Omrani are thanked for critically reading a revised version of the manuscript and providing constructive comments.

References

Aftabi, A.H., Atapour, 2000. Regional aspects of shoshonitic volcanism in Iran. Episodes 23, 119–125.
Agard, P., Omrani, J., Jolivet, L., Mouthereau, F., 2005. Convergence history across Zagros (Iran): constraints from collisional and earlier deformation. International Journal of Earth Sciences 94, 401–419.
Ahmadi-Khaladj, A., Esmaiely, D., Valizadeh, M.V., Rahimpour-Bonab, H., 2007. Petrology and geochemistry of the granitoid complex of Boroujeerd, Sanandaj–Sirjan Zone, Western Iran. Journal of Asian Earth Sciences 29, 859–877.
Alavi, M., 1994. Tectonics of Zagros Orogenic belt of Iran, new data and interpretation. Tectonophys 229, 211–238.
Allen, M.B., Jones, S., Ismail-Zadeh, A., Simmons, M., Anderson, L., 2002. Onset of subduction as the cause of rapid Pliocene–Quaternary subsidence in the south Caspian basin. Geology 30, 775–778.
Allen, M., Ghassemi, M.R., Shahrabi, M., Qorashi, M., 2003. Accommodation of late Cenozoic oblique shortening in the Alborz range, northern Iran. Journal of Structural Geology 25, 659–672.
Ashrafi, R., 2003. Geochemistry and petrology of mafic volcanic rocks from little Damavand and its comparison with trachyandesites. M. Sc. Thesis. University of Tehran (in Farsi). Asudeh, I., 1982. Seismic structure of Iran from surface and body wave data, Geophysical Journal Royal Astronomy Society 71, 715–730.
Asudeh, I., 1982. Seismic structure of Iran from surface and body wave data. Geophysical Journal Royal of Astronomy Society 71, 715–730.
Axen, G.H., Lam, P.S., Grove, M., Stokli, D.F., Hassanzadeh, J., 2001. Exhumation of the west-central Alborz mountain, Iran: Caspian subsidence, and collision-related tectonics. Geology 29, 559–562.
Beberian, F., Beberian, M., 1981. Tectono-plutonic episodes in Iran. Geological Survey of Iran, Report 52, pp. 566–593.
Berberian, M., King, G.C.P., 1981. Towards a paleogeography and tectonic evolution of Iran. Canadian Journal of Earth Sciences 18, 210–265.
Bina, M.M., Bucur, I., Pervot, M., Meyerfeld, Y., Daly, L., Cantagrel, J.M., Mergoil, J., 1986. Palaeomagnetism petrology and geochronology of Tertiary magmatic and sedimentary units from Iran. Tectonophysics 121, 303–329.
Boyd, O.S., Jones, C.H., Sheehan, A.F., 2004. Foundering lithosphere imaged beneath the southern Sierra Nevada, California, USA. Science 305, 660–662.
Braud, J., Ricou, L.E., 1971. L'accident du Zagros ou Main Thrust un charriage et un coulissement. Comptes Rendus de l'Académie des Sciences 272, 203–206.
Brousse, R., Moine-Vaziri, H., 1982. L'association shoshonitique du Damavand (Iran). Geologische Rundschau 71, 687–702.
Cousens, B.L., 1996. Magmatic evolution of Quaternary mafic magmas at Long Valley Caldera and the Devils Postpile, California: effects of crustal contamination on lithospheric mantle-derived magmas. Journal of Geophysical Research 101, 27673–27689.
Cousens, B.L., Clague, D.A., Sharp, W.D., 2003. Chronology, chemistry and origin of trachyites from Hualalai volcano, Hawaii. Geochemistry, Geophysics, Geosystems 4, 1–27.
Davidson, J.P., 1996. Deciphering mantle and crustal signatures in subduction zone magmatism. In: Bebout, G.E., Scholl, D.W., Kibery, S.H., Platt, J.P. (Eds.), Subduction: top to bottom: American Geophysical Union, 96, pp. 251–262.
Davidson, J.P., Hassanzadeh, J., Berzins, R., Stockli, F., Bashukooh, B., Turrin, B., Padamouz, A., 2004. The geology of Damavand Volcano, Alborz Mountains, Northern Iran. Geological Society of America Bulletin 116, 16–29.
Davies, J.H., Blanckenburg, V.F., 1995. Slab breakoff: a model of lithosphere detachment and its test in the magmatism and deformation of collisional orogeneses. Earth and Planetary Science Letters 129, 85–102.
Dehghani, G., Makris, J., 1984. The gravity field and crustal structure of Iran. Neues Jahrbuch für Geologie and Palaeontologie Abhundlungen 168, 215–229.
DePaolo, D.J., 1981. Trace element and isotopic effects of combined wallrock assimilation and fractional crystallization. Earth and Planetary Science Letters 53, 189–202.
Dickinson, W.R., Hatherton, T., 1967. Andesitic volcanism and seismicity around the Pacific. Science 157, 801–803.
Dodge, F.C.W., Calk, L.C., Kistler, R.W., 1986. Lower crustal xenoliths, Chinese Peak lava flow, central Sierra Nevada. Journal of Petrology 27, 1277–1304.
Doloei, J., Roberts, R., 2003. Crust and uppermost mantle structure of Tehran region from analysis of teleseismic P-waveform receiver functions. Tectonophysics 364, 115–133.
Ducea, M., 2001. The California arc: thick granitic batholiths, eclogitic residues, lithospheric-scale thrusting, and magmatic flare-ups. GSA Today 11, 4–10.
Ducea, M., Saleeby, J., 1998. A case for delamination of the deep batholithic crust beneath the Sierra Nevada, California. In: Ernst, W.G., Nelson, C.A. (Eds.), Integrated earth and environmental evolution of the southwestern United States. International Book Series, 1. Geological Society of America, and Columbia, Maryland, Bellweather, pp. 273–288.
Eiler, J.M., 2001. Oxygen isotope variations of basaltic lavas and upper mantle rocks. In: Valley, J.W., Cole, D.R. (Eds.), Stable isotope geochemistry. Mineralogical Society of America: Reviews in Mineralogy and Geochemistry, 43, pp. 319–364.
Eiler, J.M., Crawford, A., Elliott, T., Farley, K.A., Valley, W., Stolper, E.M., 2000. Oxygen isotope geochemistry of ocean-arc lavas. Journal of Petrology 41, 229–256.
Elkins-Tanton, L.T., Grove, T.L., 2003. Journal of Geophysical Research 108, 9–15.
Farmer, G.L., Glazner, A.F., Manley, C.R., 2002. Did lithospheric delamination trigger late Cenozoic potassic volcanism in the southern Sierra Nevada, California. Geological Society of America Bulletin 114, 754–782.
Feeley, T.C., 2003. Origin and tectonic implications of across-strike geochemical variations in the Eocene Absaroka volcanic province, United States. Journal of Geology 111, 329–346.
Feldstein, S.N., Lange, R.A., 1999. Pliocene potassic magmas from the Kings River region, Sierra Nevada, California: evidence for melting of a subduction-modified mantle. Journal of Petrology 40, 1301–1320.
Gao, S., Rudnick, R.L., Carlson, R.W., McDonough, W.F., Liu, Y.S., 2002. Re–Os evidence for replacement of ancient mantle lithosphere beneath the North China craton. Earth and Planetary Science Letters 198, 307–322.
Gill, J.B., Williams, R.W., 1992. The isotope and U-series studies II: subduction-related volcanic rocks. Geochimica et Cosmochica Act 54, 1427–1442.
Guest, B., Guest, A., Axen, F., 2007. Late Tertiary tectonic evolution of northern Iran: a case for simple crustal folding. Global and Planetary Change 58, 435–453.
Gutscher, M.A., Spakman, W., Bijwaar, H., Engdahl, E.R., 2000. Geodynamics of flat subduction: seismicity and tomographic constraints from the Andean margin. Tectonics 19, 814–833.
Hassanzadeh, J., Omidian, S., Davidson, J., 2006. A late Pliocene tectonic switch from transpression to transtension in the Haraz sector of central Alborz: implications for the origin of Damavand volcano. Philadelphia Annual Meeting. Paper No. 171-28. Geological Society of America.
Hawkesworth, C.J., Kempton, P.D., Rogers, N.W., Ellam, R.M., Calsteren, P.W., 1990. Continental mantle lithosphere, and shallow level enrichment processes in the Earth's mantle. Earth and Planetary Science Letters 96, 256–268.
Hollinsworth, J., Jackson, J., Walker, R., Nazar, H., 2008. Extrusion tectonics and subduction in the eastern South Caspian region since 10 Ma. Geology 36, 763–766.
Jackson, J., Priestley, K., Allen, M., Berberian, M., 2002. Active tectonics of the south Caspian basin. Geophysical Journal International 148, 214–245.
Jung, D., Kuersten, M.O.C., Tarkian, M., 1976. Post-Mesozoic volcanism in Iran and its relation to the subduction of the Afro-Arabian under the Eurasian Plate. In: Pilger, A., Roesler, A. (Eds.), Afar between Continental and Oceanic Rifting, 2, pp. 175–181.
Kay, R.W., Kay, S.M., 1993. Delamination and delamination magmatism. Tectonophysics 219, 177–189.
Keskin, M., 2003. Magma generation by slab steepening and breakoff beneath a subduction–accretion complex: an alternative model for collision-related volcanism in Eastern Anatolia, Turkey. Geophysical Research Letters 30, 9-1–9-4.
Lee, C.T., Rudnick, R.L., Brimhall Jr., G.H., 2001. Deep lithospheric dynamics beneath the Sierra Nevada during the Mesozoic and Cenozoic as inferred from xenolith petrology. Geochemistry, Geophysics, Geosystems 2 doi: 2001GC000152.
Liotard, J.M., Dautria, J.M., Bisch, D., Condomines, J., Mehdizadeh, H., Ritz, J.F., 2008. Origin of the absarokite–banakite association of the Damavand volcano (Iran): trace elements and Sr, Nd, Pb isotope constraints. International Journal of Earth Sciences 97, 89–102.
Manley, C.R., Glazner, A.F., Farmer, G.L., 2000. Timing of volcanism in the Sierra Nevada of California: evidence for Pliocene delamination of the batholithic root? Geology 28, 811–814.
Mattey, D., Lowry, D., MacPherson, C., 1994. Oxygen isotope composition of mantle peridotite. Earth and Planetary Science Letters 128, 231–241.
McDonough, W.F., Sun, S.S., 1995. Composition of the Earth. Chemical Geology 120, 223–253.
McKenzie, D., 1989. Some remarks on the movement of small melt fractions in the mantle. Earth and Planetary Science Letters 95, 53–72.
Mehdizadeh, H., Liotard, J.M., Dautria, J.M., 2002. Geochemical characteristics of an intracontinetnal shoshonitic association: the example of the Damavand volcano, Iran. Comptes Rendus Geoscience 334, 111–117.
Menzies, M.A., Hawkesworth, C.J., 1987. Mantle Metasomatism. Academic Press, London.
Motazedian, D., 2006. Region-specific key seismic parameters for earthquakes in northern Iran. Bulletin of the Seismological Society of America 96, 1383–1395.
Murphy, D.T., Collerson, K.D., Kamber, B.S., 2002. Lamproites from Gaussberg, Antarctica, possible transition zone melts of Archean subducted sediments. Journal of Petrology 43, 981–1001.
Murphy, J.B., Hynes, A.J., Johnston, S.T., Keppie, J.D., 2003. Reconstructing the ancestral Yellowstone plume from accreted seamounts and its relationship to flat-slab subduction. Tectonophysics 365, 185–194.

Nazari, H., 2006. Analyse de la tectonique récente et active dans l'Alborz Central et la région de Téhéran: « Approche morphotectonique et paléoseismologique ». PhD Thesis, Montpellier II, Montpellier, 247 pp.
Omidian, S., 2007. Structural and geochemical studies of evaluating tectonic setting of Damavand volcano. M. Sc. thesis. University of Tehran (in Farsi).
Omrani, J., 2008. The geodynamic evolution of Zagros: Tectonic and petrological constraints from the internal zones, Paris 6, Paris, 226 pp.
Omrani, J., Agard, P., Whitechurch, H., Benoit, M., Prouteau, G., Jolivet, L., 2008. Arc-magmatism and subduction history beneath the Zagros Mountains, Iran: a new report of adakites and geodynamic consequences. Lithos 106, 380–398.
Omrani, J., Agard, P., Whitechurch, H., Benoit, M., Prouteau, G., Jolivet, L., 2009. Reply to: Comment by Aftabi and Atapour on « Arc magmatism and subduction history beneath the Zagros Mountains, Iran: A new report of adakites and geodynamic consequences ». Lithos 113, 847–849.
Pandamouz, A., 1998. A new investigation of stratrigraphic position of the basaltic flows in the volcanic sequence of Damavand (central Alborz, northern Iran). M. Sc. thesis. University of Tehran (in Farsi).
Pearce, J.A., 1982. Trace element characteristics of lavas from destructive plate boundaries. In: Thorpe, R.S. (Ed.), Andesites. John Wiley and Sons, Chichester, New York.
Pineau, F., Semet, M.P., Grassineau, N., Okrugin, V.M., Javoy, M., 1999. The genesis of the stable isotope (O, H) record in arc magmas: the Kamtchatka's case. Chemical Geology 135, 93–124.
Plank, T., Langmuir, C.H., 1998. The chemical composition of subducting sediment and its consequences for the crust and mantle. Chemical Geology 145, 325–394.
Proteau, G., Scaillet, B., Pichavant, M., Maury, R., 2001. Evidence for mantle metasomatism by hydrous silicic melts derived from subducted oceanic crust. Nature 140, 197–200.
Rajaee, A.H., Mokhtari, M., Priestley, K., Hatzfeld, D., 2010. Variation of moho depth in the Central Alborz. Scientific Quarterly Journal (GSI) 16 (64).
Reagan, M.K., Gill, J.B., 1989. Coexisting calcalkaline and high-niobium basalts from turrialba volcano, Costa Rica: implications for residual titanates in arc magma sources. Journal of Geophysical Research 94, 4619–4633.
Rehkamper, M., Hofmann, A.W., 1997. Recycled ocean crust and sediment in Indian Ocean MORB. Earth and Planetary Science Letters 147, 93–106.
Ritz, J.F., Nazar, H., Ghasemi, A., Salamati, R., Shafei, A., Solaymani, S., Vernant, P., 2006. Active transtension inside central Alborz: a new insight into northern Iran–southern Caspian geodynamics. Geology 34, 477–480.
Sengör, A.M.C., Cin, A., Rowley, D.B., Nie, S.Y., 1993. Space–time patterns of magmatism along the Tethysides: a preliminary study. Journal of Geology 101, 51–84.
Shafiei, B., Haschke, M., Shahabpour, J., 2009. Recycling of orogenic arc crust tiggers porphyry Cu mineralization in Kerman Cenozoic arc rocks, southeastern Iran. Mieralum Deposita 44, 265–283.
Sodoudi, F., Yuan, X., Kind, R., Heit, B., Sadidkhouy, A., 2009. Evidence for a missing crustal root and a thin lithosphere beneath the Central Alborz by receiver function studies. Geophysics Journal International 177, 733–742.
Stacey, J.S., Kramers, J.D., 1975. Approximation of terrestrial lead isotope evolution by a two – stage model. Earth and Planetary Science Letters 26, 207–221.
Stöcklin, J., 1968. Structural history and tectonics of Iran: a review. American Association of Petroleum Geologists Bulletin 52 (7), 12229–12580.
Tainton, K.M., McKenzie, D., 1994. The generation of kimberlites, lamproites and their source rocks. Journal of Petrology 35, 787–817.
Taylor, B.E., 2004. Fluorination methods in stable isotope analysis. In: de Groot, Pier A. (Ed.), Handbook of Stable Isotope Analytical Techniques, pp. 400–472.
van Kooten, G.K., 1980. Mineralogy, petrology, and geochemistry of an ultrapotassic basaltic suite, central Sierra Nevada, California, USA. Journal of Petrology 21, 651–684.
Verdel, C., 2009. Cenozoic geology of Iran: an integrated study of extensional tectonics and related volcanism. Ph. D. thesis. California Institute of Technology. 287 pp.
Vernant, P.h., Nilforoushan, F., Chéry, F., Bayer, R., Djamour, Y., Masson, F., Nankali, H., Ritz, J.F., Sedighi, M., Tavakoli, F., 2004. Deciphering oblique shortening of central Alborz in Iran using geodetic data. Earth and Planetary Science Letters 223, 177–185.
Weaver, B.L., 1991. The origin of ocean island basalt end-member compositions: trace element and isotopic constraints. Earth and Planetary Science Letters 104, 381–397.
Wernicke, B., et al., 1996. Origin of high mountains in the continents: the southern Sierra Nevada. Science 271, 190–193.
Wilson, M., 2001. Igneous Petrogenesis. A Global Tectonic Approach. Chapman and Hall, UK.
Wood, D.A., 1980. The application of a Th–Hf–Ta diagram to problems of tectono-magmatic classification and to establishing the nature of crustal contamination of basaltic lavas of the British Tertiary volcanic province. Earth and Planetary Science Letters 50, 11–30.
Workman, R.K., Hart, S.R., 2005. Major and trace element composition of the depleted MORB mantle (DMM). Earth and Planetary Science Letters 231, 53–72.
Zanchi, A., Berra, F., Mattei, M., Ghassemi, M.R., Sabouri, J., 2006. Inversion tectonics in central Alborz, Iran. Journal of Structural Geology 28, 2023–2037.
Zandt, G., Gilbert, H., Owens, T.J., Ducea, M., Saleeby, J.B., Jones, C.H., 2004. Active foundering of a continental arc root beneath the southern Sierra Nevada in California. Nature 431, 41–46.